Electronic structure of Cu_2O and CuO

J. Ghijsen, L. H. Tjeng, J. van Elp, H. Eskes,
J. Westerink, and G. A. Sawatzky
Department of Solid State and Applied Physics, Material Research Centre, University of Groningen, Nijenborgh 18, NL-9747 AG Groningen, The Netherlands

M. T. Czyzyk
ESM Afdeling, Fakulteit der W & N, Catholic University of Nijmegen, Toernooiveld, NL-6525 ED Nijmegen, The Netherlands

(Received 25 July 1988)

The electronic structure of copper oxides has been investigated by photoelectron (x-ray photoemission, ultraviolet photoemission), Auger electron, and bremsstrahlung isochromat spectroscopies. The experimental results are compared with one-electron band-structure calculations as well as with a cluster configuration interaction model. It is demonstrated that the results for Cu_2O agree well with band theory, whereas those for CuO clearly show strong deviations which we argue are due to electron-correlation effects in the open-shell d bands. From the comparison to cluster calculations we extract values for the Cu d-d and O p-p Coulomb interactions, the O to Cu charge transfer energy, and the degree of Cu d-O $2p$ hybridization. From this we demonstrate that CuO is a charge-transfer gap insulator.

I. INTRODUCTION

Cu_2O and CuO are almost ideal compounds to study the influence of electron-correlation effects on the electronic structure of transition-metal compounds in general and the high-T_c superconductors in particular. The crystallographic structure of Cu_2O is highly symmetric with six atoms per unit cell: the oxygen atoms form a bcc lattice, while the copper atoms are on the vertices of a tetrahedron around each oxygen atom. This is one of the rare occurrences of linear O-Cu-O coordination.[1] In CuO the lattice has a monoclinic symmetry.[2] Each atom has four nearest neighbors of the other kind: copper atoms are at the center of an oxygen rectangle, while oxygen atoms are at the center of a copper distorted tetrahedron. Band-structure calculations became available only very recently for CuO,[3,4] whereas many band-structure calculations of Cu_2O exist in the literature.[5-8] Crystallographic parameters and interatomic distances to nearest neighbors are listed in Table I.

TABLE I. Crystallographic parameters (from Refs. 1 and 2).

	Cu_2O	CuO
Lattice parameter	Cubic $a=4.27$ Å	Monoclinic $a=4.6837$ Å $b=3.4226$ Å $c=5.1288$ Å $\beta=99.54°$
Shortest distances		
$d_{Cu\text{-}O}$	1.84 Å	1.95 Å
$d_{O\text{-}O}$	3.68 Å	2.62 Å
$d_{Cu\text{-}Cu}$	3.02 Å	2.90 Å

Cu_2O is expected to have an essentially full Cu $3d$ shell. It forms a much studied textbook example of a semiconductor with a gap of 2.17 eV.[9] Because of the full $3d$ shell, band theory using the ground-state charge density is expected to provide a good description of the electronic structure (except perhaps for a smaller band gap) and related photoemission spectroscopy (PES) and bremsstrahlung isochromat spectroscopy (BIS) spectra since the hole created in PES and the electron created in BIS have no open-shell $3d$ holes or electrons to correlate with. This situation is somewhat similar to Cu metal for which band theory gives a very successful description of the electronic structure.[10]

CuO has an open d shell ($3d^9$) and is an (antiferromagnetic) semiconductor with a gap of about 1.4 eV,[11] whereas band theory predicts it to be metallic for reasons which are probably similar to the failure of band theory in NiO and CoO.[12,13] On the other hand, this absence of gap may result at least partially from the approximation still involved in the band-structure calculation (see some further discussion of this aspect in Ref. 3). It is of great interest to determine the influence of the open $3d$ shell on the band structure and especially the ionization states as measured by PES and to determine the magnitude of the $3d$ electron-electron interaction since the basic structural unit is similar to the CuO_2 layers in the high-T_c superconductors.

Although several x-ray photoemission spectroscopy [14-17] (XPS) and some Auger[17] and photon-energy-dependent ultraviolet photoemission spectroscopy[18,19] (UPS) measurements on these oxides have been reported, there is no published work on BIS (Ref. 20) or a comparison of UPS (He I or He II) to band-structure calculations. We mention here that the Cu $L_{2,3}M_{4,5}M_{4,5}$ Auger spectroscopy on Cu_2O should have a fairly straightforward interpretation similar to that of Cu metal[21] and,

therefore, the *d-d* Coulomb interaction can be directly determined from the relation

$$U_{\text{eff}} = E_{\text{kin}} - E_b(2p) - 2E_b(3d) , \quad (1)$$

where $E_b(2p)$ is the Cu $2p$ binding energy and $E_b(3d)$ is the binding energy of a $3d^9$ state both of which are determined from PES. We note also that Cu $3d^8$-like states are reached by an $L_{2,3}M_{4,5}M_{4,5}$ Auger process in Cu_2O whereas in CuO they can be reached by one-electron ionization as in photoemission since the ground state already contains *d* holes. In a sense, going from Cu_2O to CuO is like going from the simplicity of Cu metal to the complexity of Ni metal when attempting to describe the electronic structure.

In this paper, we present combined photoemission, BIS, and Auger data for Cu_2O and CuO and compare them with the results obtained using an extended basis set within the localized augmented-spherical-wave (ASW) method.[3,22] We conclude that the Cu $3d$ Coulomb interaction is larger than the O $2p$-Cu $3d$ charge transfer energy Δ in CuO making CuO a charge transfer semiconductor of type *B* in the phase diagram of Zaanen, Sawatzky, and Allen (ZSA).[23,24]

II. SAMPLE PREPARATION AND EXPERIMENTAL SETUP

The samples were prepared starting with 99.999%-pure copper. The metal surface was sandpaper roughened before introduction into the spectrometer. In a first step, copper was sputter cleaned until a clean XPS spectrum was obtained. Thereafter, the valence-band spectrum was recorded to determine the position of the Fermi level which was subsequently used as the reference of binding energies. The oxidation of Cu under 1-Torr O_2 (99%) at 400 °C for 1.5 h produced a CuO layer thick enough to conceal the underlying metal from XPS and UPS, but thin enough to allow for a good compensation of the charging effect. Cu_2O was produced by heating CuO *in vacuo* at 300 °C for about 1 h. During the conversion from CuO to Cu_2O, Cu $2p$ spectra were continuously measured to monitor the disappearance of the Cu $2p$ satellite which is a fingerprint of CuO.[17]

XPS and BIS measurements were performed using a modified Auger electron infrared (AEI) 200 spectrometer, with a residual gas pressure in the low 10^{-10}-Torr range. The XPS source was the unmonochromatized Al $K\alpha$ line (1486.7 eV), which corresponds also to the energy of the photons collected by BIS. The instrumental broadening is estimated to be 1.0 for XPS and 0.7 eV for BIS. UPS data were collected using an ADES 400 spectrometer, with a base pressure better than 10^{-10} Torr. The resolution was 0.25 eV for He II and 0.1 eV for He I.

BIS measurements are more severely plagued by charging effects than for XPS, because the electron current is quite high (typically 200 μA vs 1 nA). This could, however, be avoided by our sample preparation procedure. Besides charging effects, another source of trouble is the possible decomposition in the electronic beam, especially of CuO. For the BIS spectra reported on here, there was no detectable decomposition as confirmed by XPS measurements before and after the BIS measurements.

III. EXPERIMENTAL RESULTS AND DISCUSSION

A. Core levels

We consider first core-level spectra of oxygen and copper (Table II), and use them to check the composition of our material. The O $1s$ spectra are displayed in Fig. 1. In CuO, a shoulder is apparent at about 1.8 eV higher binding energy from the main peak. This is similar to the observation by Robert, Bartel, and Offergeld[15] who attri-

TABLE II. Core-level binding energies (eV).

Cu $2p_{3/2}$			O $1s$		
Cu	Cu_2O	CuO	Cu_2O	CuO	Reference
932.3 ± 0.1	932.4 ± 0.2	933.2 ± 0.2	530.2 ± 0.2	529.2 ± 0.3	This work
	932.2	933.6	530.4	529.7	a
	932.2	933.2	530.5	529.9	b
	933.0		531.0	530.7	c
932.4	932.5	933.8		529.5	d
932.5	932.5	933.8	530.5	529.6	e
	932.0	933.5	529.9	529.5	f
932.5					g
932.2					h

[a]Reference 15.
[b]K. Hirokawa, F. Honda, and M. Oku, J. Electron. Spectrosc. **6**, 333 (1975).
[c]T. Novakov and R. Prins, Solid State Commun. **9**, 1975 (1971).
[d]T. H. Fleisch and G. J. Mains, Appl. Surf. Sci. **10**, 51 (1982).
[e]N. S. McIntyre and M. G. Cook, Anal. Chem. **47**, 2208 (1975).
[f]N. Nücker, J. Fink, B. Renker, D. Ewert, C. Politis, P. J. W. Weijs, and J. C. Fuggle, Z. Phys. B **67**, 9 (1987).
[g]J. C. Fuggle and N. Mårtensson, J. Electron. Spectrosc. **21**, 275 (1980).
[h]Reference 21.

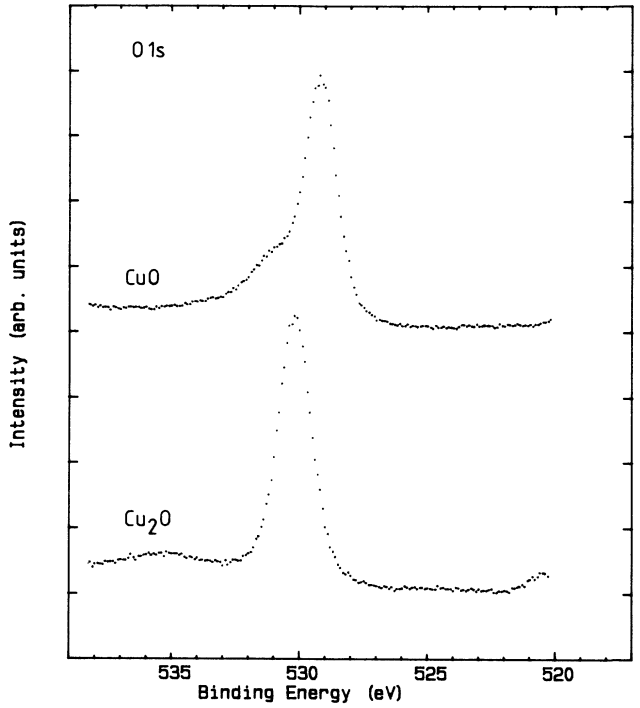

FIG. 1. O 1s spectra normalized to the peak height. The shoulder observed on the high-binding-energy side results from contamination. Bottom, Cu_2O; top, CuO.

buted it to hydroxide and/or chemisorbed oxygen. The binding energies are 529.2 ± 0.3 and 530.2 ± 0.2 eV for CuO and Cu_2O, respectively.

The Cu $2p_{3/2}$ peaks are shown in Fig. 2 and exhibit the known characteristics of CuO and Cu_2O. The main peak of CuO is relatively broad (3.4 eV), has a binding energy

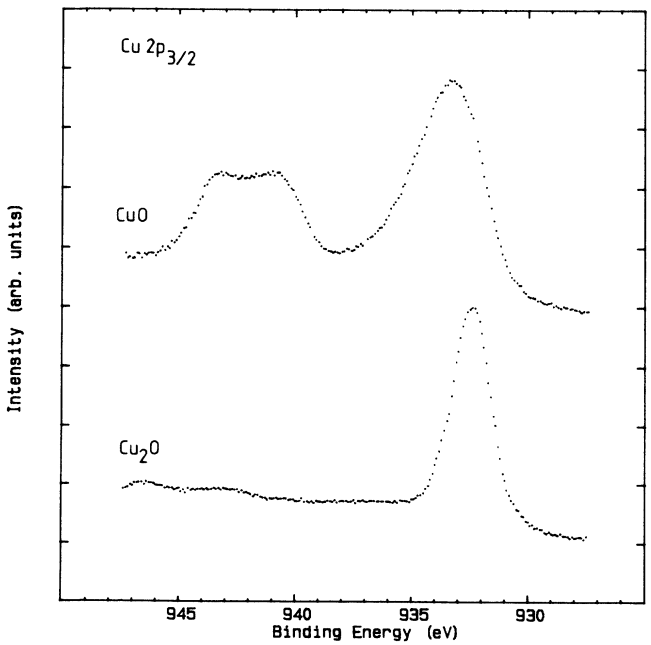

FIG. 2. Cu $2p_{3/2}$ spectra, normalized to the peak height. Bottom, Cu_2O; top, CuO.

of 933.2 ± 0.2 eV, and is accompanied by a satellite on the high-binding-energy side at about 9 eV. This satellite is characteristic of materials having a d^9 configuration in the ground state, such as, e.g., the copper dihalides[25] or metallic nickel.[26] The structure seen in the satellite line is due to the multiplet splitting in the $2p^5 3d^9$ final state (note that the very existence of this multiplet structure supports the assignment of $2p^5 3d^9$ to the satellite and not to the main peak as was originally proposed by Kim[16]). The spectrum of Cu_2O has only one peak at 932.4 ± 0.2 eV, which is significantly narrower (1.9 eV).

A simple model explaining the physical origin of the satellite in CuO and its absence in Cu_2O is based on a cluster approach as used for the copper and nickel dihalides.[25,27,28] In this model, the ground state for CuO is approximated by

$$\Psi_G = \cos\theta\,|\,d^9\rangle - \sin\theta\,|\,d^{10}\underline{L}\rangle\,, \tag{2}$$

where $|\,d^9\rangle$ and $|\,d^{10}\underline{L}\rangle$ are configurations involving either $d(|\,d^9\rangle)$ or ligand (O $2p$) holes ($|\,d^{10}\underline{L}\rangle$). Using T as the transfer integral,

$$T = \langle d^9\,|\,H\,|\,d^{10}\underline{L}\rangle\,, \tag{3}$$

where H is the Hamiltonian, and a charge transfer energy

$$\Delta = E(d^{10}\underline{L}) - E(d^9)\,, \tag{4}$$

we find $\tan(2\theta) = 2T/\Delta$. In the states with the core hole present, the $|\,d^{10}\underline{L}\rangle$ configuration is pulled down relative to the $|\,d^9\rangle$ configuration by the core hole—$3d$ interaction Q. The resulting final states can be written as

$$\begin{aligned} \Psi_M &= \cos\theta'\,|\,\underline{c}d^9\rangle - \sin\theta'\,|\,\underline{c}d^{10}\underline{L}\rangle\,, \\ \Psi_S &= \sin\theta'\,|\,\underline{c}d^9\rangle + \cos\theta'\,|\,\underline{c}d^{10}\underline{L}\rangle\,, \end{aligned} \tag{5}$$

where the subscripts M and S refer to the main peak and satellite, respectively, $\tan(2\theta') = 2T/(\Delta - Q)$. The energy separation is given by

$$W = E_S - E_M = [(\Delta - Q)^2 + 4T^2)]^{1/2}\,. \tag{6}$$

The satellite to main line intensity ratio is in the sudden approximation given by

$$I_S/I_M = |\langle\Psi_M\,|\,\Psi_G\rangle|^2 / |\langle\Psi_S\,|\,\Psi_G\rangle|^2 = \tan^2(\theta - \theta')\,. \tag{7}$$

The average energy separation is 9 eV and the intensity ratio is 0.55. Using these values and $Q = 9$ eV as found for the copper dihalides, we find $\Delta = 1.55$ eV and $T = 2.5$ eV. Both Δ and T are considerably larger than the values found by Shen *et al.*[29] which were also based on valence-band spectroscopy. Using methods defined in Ref. 24, these values together with an U_{dd} of 8 or 9 eV result in a band gap of 1.7 eV somewhat larger than the experimentally determined gap. As pointed out by Zaanen *et al.*[27] this discrepancy could be due to an oversimplification of the influence of the core hole as well as to the neglect of the O $2p$ bandwidth.

Within this cluster model, the d shell of Cu_2O is full so that screening via a charge transfer into the d states is not possible. The screening of the core hole must then be accomplished by states involving the broad sp conduction

band and will, therefore, not yield sharp satellite structures.

B. Auger spectroscopy

Unfortunately the *d-d* correlation energy U cannot be determined from core-level spectroscopies because the d^8 states are not involved. For this purpose, however, Auger spectroscopy can be used. The O *KLL* and Cu *LMM* Auger spectra are displayed in Figs. 3 and 4. The energy they are referred to is the energy of the Auger electron above the Fermi energy in the solid. This energy shall later be compared to the value derived from the binding energies of the levels involved, to estimate the correlation energies of the outer-shell electrons. Comparing the oxygen Auger spectra of CuO and Cu_2O we notice that the CuO spectrum is extremely wide. This is probably a result of the O $2p$ valence-band spectral weight being spread out over a much broader energy range in CuO than Cu_2O. This, as we will see below, is supported both by band-structure calculations and by energy-dependent photoelectron spectroscopy.

Also, the Cu $L_3M_{4,5}M_{4,5}$ spectra of CuO and Cu_2O show distinct differences. For Cu_2O in which the ground state is nominally d^{10}, the two-hole final state after Auger decay is primarily $3d^8$ which splits in various multiplet states corresponding to structures seen between 916 and 919 eV.[21] This multiplet spread is, however, too small to explain the structure seen at about 922 and 910–914 eV. The structure at 922 eV is most likely a result of final-state hybridization with the states $d^9\underline{L}$ which lie about 5–6 eV lower in energy than the Cu d^8 states as we will see below. The structure at lower kinetic energy is primarily due to Coster-Kronig-preceded Auger transitions

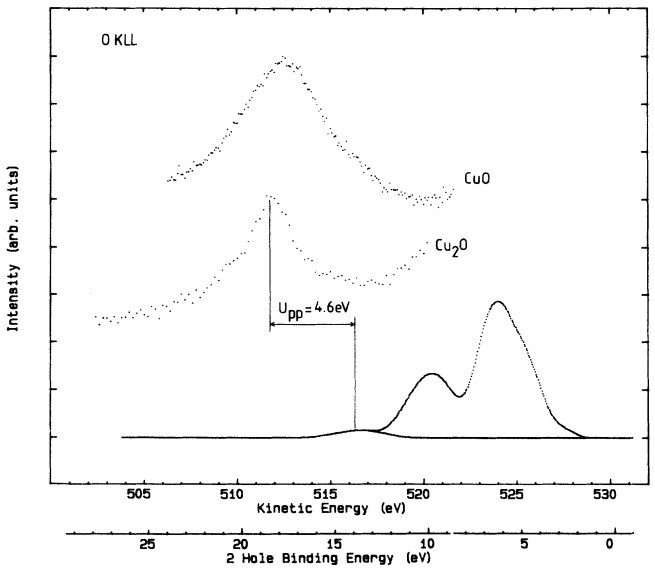

FIG. 3. O *KLL* Auger spectra, normalized to the peak height. Top, CuO; middle, Cu_2O. The bottom curves show the self-convolution of Cu_2O He II valence-band spectra, for the full valence band, and for the O $2p$ part ($5 < E_b < 9$ eV). The two-hole binding-energy scale applies to Cu_2O only.

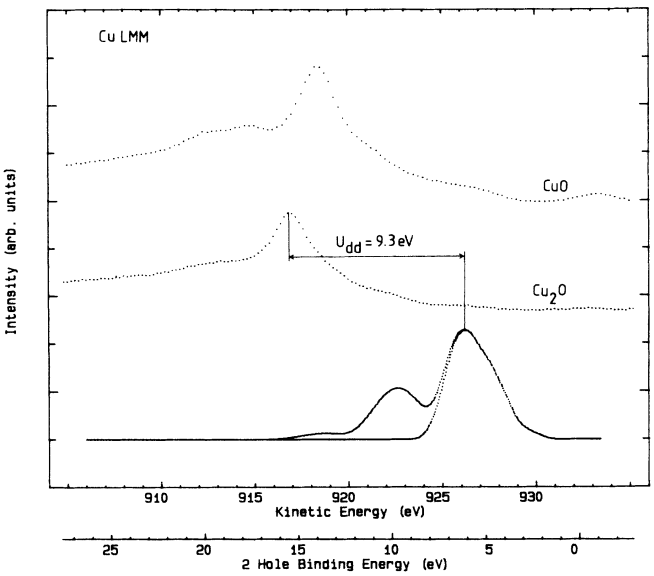

FIG. 4. Cu $L_3M_{4,5}M_{4,5}$ Auger spectra, normalized to the peak height. Top, CuO; middle, Cu_2O. The bottom curves show the self-convolution of Cu_2O He II valence band, for the full valence band, and for the Cu $3d$ part ($E_b < 5$ eV). The two-hole binding energy scale applies only to Cu_2O.

originating from the L_2 level.[30]

The Auger spectral shape for CuO is considerably different from that of Cu_2O. In fact, we expect the CuO spectrum to be quite complicated because it can originate from the $2p$ main line ($2p^5 3d^{10}\underline{L}$) after which the final state would be nominally $d^8\underline{L}$ or it could originate from the satellite ($2p^5 d^9$) for which the final state would be nominally d^7. The $d^8\underline{L}$ and the d^7 states are separated by about $2U-\Delta$ but the source energy for the d^7 state is about 9 eV larger so that we expect, for $U \approx 9$ eV and $\Delta \approx 2$ eV, the d^7 structure to occur at about 7 eV lower kinetic energy. Unfortunately, this structure occurs at about the same energy region as the previously mentioned Coster-Kronig-preceded Auger structure ($d^7\underline{L}$) so a detailed analysis is not possible. Because of this complication in CuO it will be difficult to extract U directly from the Auger spectra.

C. Valence bands

Valence-band spectra measured with different light sources are displayed in Figs. 5 and 6 for Cu_2O and CuO, respectively. In the case of XPS and He II, they are compared with calculated densities of states (DOS), broadened as explained in Table III. The binding energies are listed in Table IV, where calculated energies have been shifted to match the first peaks. Utilizing the known energy dependence of the photoionization cross section we can easily identify regions of primarily O $2p$ or Cu $3d$ spectral weight. The cross-section ratios are σ(O $2p$)/σ(Cu $3d$) $\approx$ 1.41, 0.69, and 0.02 for $h\nu$ = 21.2 (He I), 40.8 (He II), and 1486.7 (Al $K\alpha$) eV, respectively.[31] Therefore, in XPS we see primarily the d spectral weight which in Cu_2O is concentrated at 1–4 eV whereas in CuO

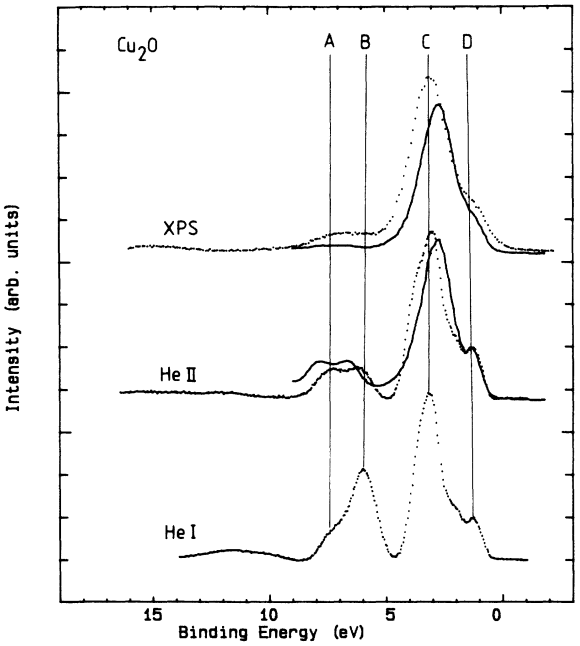

FIG. 5. Valence-band spectra from Cu_2O. Bottom, He I; middle, He II; and top, XPS. Intensities are normalized to the peak height. The solid lines superimposed on XPS and He II data are broadened d DOS and total DOS curves, respectively, using broadenings from Table III.

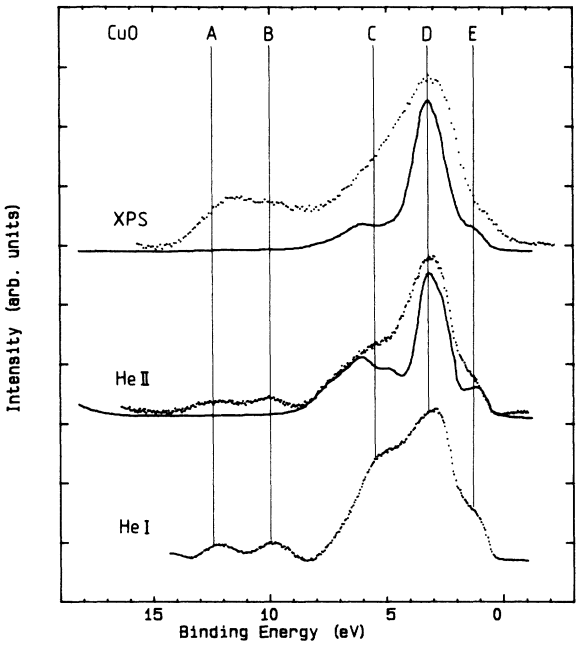

FIG. 6. Valence-band spectra from CuO. Bottom, He I; middle, He II; and top, XPS. Intensities are normalized to the peak height. The solid lines superimposed on XPS and He II data are broadened d DOS and total DOS curves, respectively, using broadening from Table III.

it is spread over a very wide energy range of 1–12 eV. Similarly, the O $2p$ character is concentrated around 6–7 eV in Cu_2O and a wide range of 1–6 eV in CuO. The shoulder seen in XPS for Cu_2O at 4–8 eV corresponds to the Cu $3d$ character in the $2p$ band due to hybridization. The structure at 8–12 eV in the CuO spectrum is due to the d^8-like final states. This is often referred to as the satellite, but it in fact is the state most directly reached by d ionization from the predominantly d^9 ground state. The large range of the spectral distribution in CuO is fairly direct evidence of strong electron-electron interactions. Also, the fact that the d^8 structure is at higher binding energy than the $d^9\underline{L}$ structure shows that $U > \Delta$, putting CuO in class B of the ZSA scheme.[23,24]

Broadened total DOS results are compared in the middle of Figs. 5 and 6 with valence-band spectra measured with He II. For He II the O $2p$ and Cu $3d$ cross sections are similar and, therefore, the spectrum should resemble the total density of states. For Cu_2O we see a good overall agreement with experiment. The major differences have to do with precise energy positions of structures. For example, the O $2p$–Cu $3d$ energy separation (peaks B and C of Table IV) is about 1.0 eV larger in the band-structure calculations than observed experimentally. This is a discrepancy also observed for other monovalent copper compounds (e.g., CuCl) (Ref. 32) and is an effect of the self-interaction energy.

The main difference for CuO is the absence of the "satellite" between 10 and 12 eV in the band-structure calculation. This becomes much more evident if we compare the partial densities of states to the experimental data in the case of XPS. We see that while the XPS spectrum of

TABLE III. Lorentzian and Gaussian broadening parameters (in eV) used for the calculation of theoretical spectra. The same values were used for Cu_2O and CuO. The Lorentzian broadening represents lifetime effects, while the Gaussian broadening represents instrumental effects.

Spectrum	Contributing partial DOS	Lorentzian (full width at half maximum)	Gaussian (full width at half maximum)
XPS	Total on Cu site	$0.25+0.1(E-E_0)$	0.7
He II	Total	$0.25+0.1(E-E_0)$	0.25
BIS	Total	$0.25\pm0.09(E-E_0)$ [a]	0.6

[a]For CuO, 0.8 was used instead of 0.25, which would produce too sharp a leading peak. This only slightly affects the shape of peaks at higher energies.

TABLE IV. Valence-band and conduction-band energies (eV). Positions are obtained from UPS data. Labels refer to Figs. 5, 6, 8, and 9.

	Cu_2O			CuO	
	Measured		Calculated		
XPS, UPS	7.3 ± 0.6	A	7.95	12.38 ± 0.22	A
	5.98 ± 0.11	B	6.70	10.02 ± 0.16	B
	3.11 ± 0.10	C	2.78	5.5 ± 0.4	C
	1.25 ± 0.09	D	1.29	3.10 ± 0.11	D
				1.23 ± 0.11	E
Gap energy	2.4 ± 0.3			1.4 ± 0.3	
BIS	3.1	W		1.8	W
	8.1	X		6.8	X
	13.4	Y		10.6	Y
				17.8	Z

Cu_2O agree very well with d partial density of states, the agreement with CuO is very poor. This is clearly due to involving two Cu $3d$ hole states in one electron removal spectrum. The description of the one-electron removal spectrum [like to the problem in NiO (Refs. 12 and 33)] apparently goes beyond the ground-state band theory.

D. Correlation energies

Combining the valence-band binding energies with those of the core levels and the Auger kinetic energies, we can use relation (1) to determine the O pp and Cu dd correlation energies. A better way is to translate the Auger spectrum into a two-hole binding energy by subtracting the core-hole binding energy and comparing this to the self-convolution of the one-hole spectral distribution. The self-convolution is obtained from the He II spectrum for which it is simple to separate the O $2p$ and Cu $3d$ regions. In Fig. 4 we see self-convolution of the main d spectral weight and in Fig. 3 that of the O $2p$ spectral weight together with the corresponding two-hole spectral distribution as obtained from Auger spectroscopy. Also indicated are the resulting Coulomb interactions $U_{pp}=4.6$ eV and $U_{dd}=9.3$ eV. The value for U_{pp} is comparable to that found in other oxides[34] and the high-T_c superconductors.[35] The U value for Cu corresponds to the dominant d^8 component reached in Auger spectroscopy which is of ^1G character, for which the relation between the U value and the Racah parameters is

$$U_{dd}(^1G)=A+4B+2C. \tag{8}$$

As is well established,[36] the multiplet splitting in the solid is nearly the same as in the free ion so the lowest-energy (^3F) d^8 state has a U value of 2.3 eV lower.[21] Although U is strongly reduced from the free-ion value [$U\approx16$ eV (Ref. 37)] because of the screening of the F^0 Slater integral it nonetheless is much larger than the d-band dispersional width in Cu_2O as we can see from Fig. 5.

Unfortunately, we cannot determine U in this way for CuO because of the complexity of the core levels, the valence bands, as well as the Auger spectrum. However, we expect the screening in CuO to be comparable to that in Cu_2O since most of the screening is due to the higher polarizability of the O^{2-} ions.[37] A rough estimate of the change in screening in going from Cu_2O to CuO can be made as follows. The screening due to polarizable ions goes to R^{-4}, where R is the nearest-neighbor distance[38] and is proportional to the number of nearest O neighbors. Using Table I, we arrive at a screening contribution for CuO which is 1.6 times that in Cu_2O. In Cu_2O the screening was found to be 7 eV, so an estimate for CuO is 11 eV resulting in a U_{dd} of 4–5 in CuO. Another estimate of the minimum value would be that of Cu metal [$U_{dd}(^1G)=7$ eV].[30]

E. Cluster model: Parameter estimates

For CuO a clear identification of the valence-band spectra with DOS features cannot be done. The high-energy "satellite" structure which we identify as being predominantly d^8 indicates a large U for CuO. Because of this, it is probably more appropriate to describe the valence electronic structure with an Anderson impurity model[23,24] or with a configuration interaction (CI) cluster-type calculation.[29] Because of the almost molecularlike structure of CuO, the electronic structure is probably well described by a $(CuO_4)^{6-}$ cluster with the copper in the center of the oxygen square (D_{4h} point group) although in the actual lattice the O ions form nearly a rectangle, with an O-Cu-O angle of 84° rather than 90° (Ref. 2). The details of such a cluster calculation will be published elsewhere. Here we suffice by specifying the basis and the interactions used. We take into account the p_x, p_y, p_z atomic orbitals on the oxygens, and the $3d$ (x^2-y^2, $3z^2-r^2$, xy, xz, yz) orbitals on Cu which have b_{1g}, a_{1g}, b_{2g}, and e_g symmetry, respectively. We considered an oxygen-oxygen transfer integral $T_{pp}=1.25$ eV chosen to agree with the bandwidth found from band theory, and $Op\rightarrow Cud$ transfer integrals as dictated by symmetry and the observation that the π transfer integrals are about half as large as the σ-type transfer integrals[39]

$$T(a_1)=T(b_1)/\sqrt{3},\quad T(b_2)=T(b_1)/2,\quad T(e)=T(b_2)/\sqrt{2}.$$

For the Cu d^8 states the Racah parameters $B=0.15$ and $C=0.58$ were taken from free-ion optical data.[37] These parameters determine the d^8 multiplet structure. $T(b_1)$, A, and Δ were taken as adjustable parameters and the d-d Coulomb interaction A used here would be equal to U if $B=C=0$ but, in fact, the "U" value one should use depends on the d^8 state considered. For example, for the $^1A_{1g}$ state in D_{4h} symmetry composed of $d(x^2-y^2)\uparrow \times d(x^2-y^2)\downarrow$, U is given by $U(^1A_{1g})=A+4B+3C$, whereas for the $^3B_{1g}$ state $d(x^2-y^2)\uparrow d(x^2-y^2)\uparrow$ one has $U(^3B_{1g})=A-8B$. For the above value of B and C these states are split by 3.5 eV which is not negligible. The full Coulomb and exchange matrices for d^8 in D_{4h} symmetry are given in Ref. 40. The configurations considered in the calculations are $|d^9\rangle$, $|d^{10}\underline{L}\rangle$ of the b_{1g},

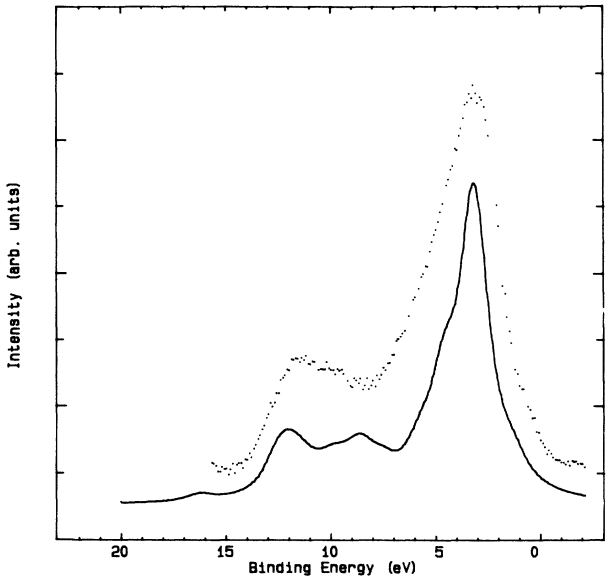

FIG. 7. XPS valence-band spectrum of CuO (dots) compared with the result obtained by the cluster calculation (solid line) described in Ref. 41.

a_{1g}, b_{2g}, or e_g symmetry for the "neutral" (ground) state; $|d^{10}\rangle$ for the electron addition state (BIS); and $|d^8\rangle$, $|d^9\underline{L}\rangle$, $|d^{10}\underline{L}^2\rangle$ for the electron removal states where again we considered all the irreducible representations spanned by two d holes in D_{4h} symmetry. The theoretical d removal spectral weight for $T(b_1)=2.3$, $\Delta=2.2$, $A=6.0$ is compared to the XPS spectrum in Fig. 7. The band gap calculated with these parameters is 1.25 eV. Since the theoretical spectra are very sensitive to the choice of parameters and since they give us the correct energy spread of the d spectral weight, we feel that these are good estimates for CuO. We can compare this value of 7.8 eV found for $U(^1G)$ applying relation (8) to Auger spectroscopy measurements of Cu_2O (9.3 eV) as found above. We see indeed that the U value for CuO is less than that for Cu_2O because of the increased screening, although the difference is less than our estimate above. The Cu $3d$ to O $2p$ transfer integral $T(b_{1g})$ is close to that found from the core-level spectral shape analysis above, whereas the value found for Δ is about 0.7 eV larger. As pointed out in Ref. 27, it is not uncommon that somewhat different parameters are found for two different spectroscopies.

Of special interest is the nature of the first shoulder in the photoemission spectrum since it describes the holes that would be induced by doping. This shoulder is of solely $^1A_{1g}$ character but has only a few percents of d^8 mixed in. It is primarily a $d^9\underline{L}$ state with one hole in a $d(x^2-y^2)$ orbital and the other in O $2p$ orbitals combining to form an orbital of b_1 symmetry. These two holes have a strong antiferromagnetic exchange as described in more detail elsewhere.[41]

F. Conduction bands: Band gaps

BIS results are displayed in Figs. 8 and 9, along with XPS spectra and DOS of unoccupied levels. The energy in both XPS and BIS is referred to the Fermi level, measured on copper prior to oxidation. The gap is found to be 2.4 eV in Cu_2O and 1.4 eV in CuO, in good agreement with previous determinations.[9,11] The DOS of Cu_2O was shifted (1.2 eV) to align it with the leading peak of the BIS. For CuO, a shift of 0.7 eV was necessary. For both compounds, a good agreement is observed between measured and calculated features. The leading peak of CuO (1.8 eV) is attributed to the completion of the $3d$ shell.

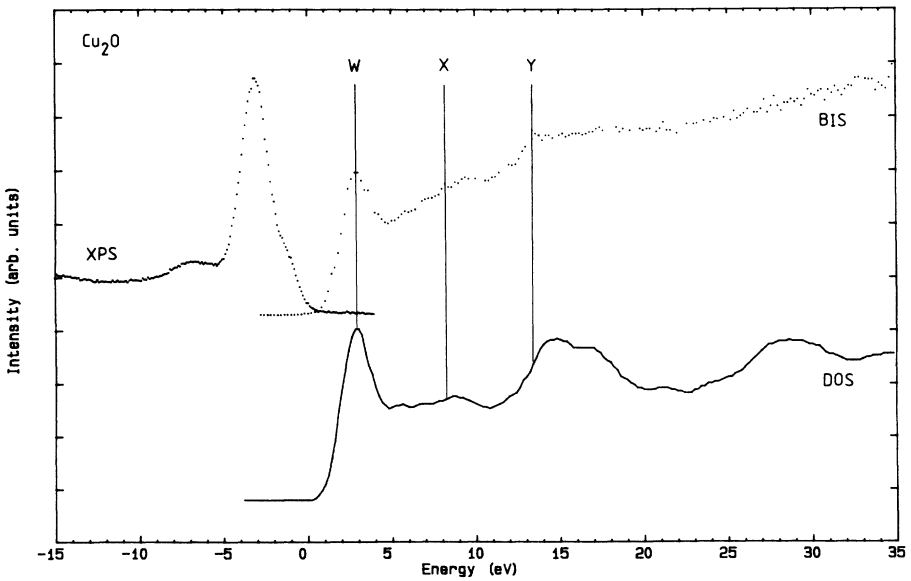

FIG. 8. XPS (dots, left-hand side), BIS (dots, right-hand side), and conduction-band density of states (solid line, right-hand side) of Cu_2O. The vertical scales of the different curves are independent. The DOS has been shifted to align the leading peak with the BIS results.

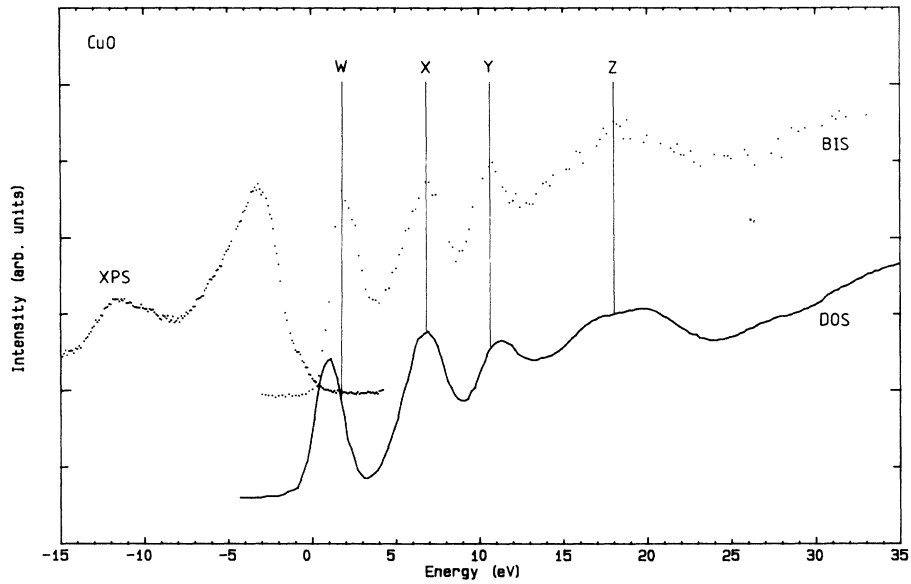

FIG. 9. XPS, BIS, and conduction-band density of states of CuO, as in Fig. 8. The DOS has been shifted to bring the second peak under its BIS counterpart.

The peaks at 6.8 and 10.6 eV correspond to the filling of empty *sp* states on copper or on oxygen, while the *d* DOS of oxygen has a peak corresponding to the one observed at 17.8 eV.[3]

In view of the intense sharp peak observed at 3.1 eV in Cu_2O, one might suspect a stoichiometry defect, giving rise to some d^9 states, whose filling would then be responsible for it. This can, however, be ruled out because the Cu 2*p* peak was measured by XPS both before and after BIS and gave a clear indication that the measured material was Cu_2O, without significant changes from the electron bombardment. Furthermore, the peak is also seen in the DOS result which is reliable for Cu_2O, due to the absence of *d* holes. The identification of peaks from the DOS is as follows: the peak at 3.1 eV corresponds to Cu *d* and O *p*, the peak at 8.1 eV is Cu *s*, and the peak at 13.4 eV is Cu *p* with some O *p* contributions. Despite the good agreement between the calculated DOS and the BIS results, there is no measured peak corresponding to the DOS peak at about 28 eV. Even if one takes into account that lifetimes broadening effects increase with the energy of the level, it is unlikely that such effects would blur that peak out completely.

At first glance, one might be surprised that band theory does so well for the BIS spectra even for CuO. However, if we accept that correlation effects are large then in the ground state the wave function is of the form

$$\Psi = \alpha \,|\, d^9\rangle + \sum \beta_k \,|\, d^{10}\underline{L}_k\rangle \tag{9}$$

with negligible d^8 character. In this case, there is only one state left for the extra electron in BIS resulting in a d^{10} state. We then do not expect any satellite structure since the electron addition produces a closed *d* shell.

Despite its limitations, the cluster configuration interaction (CI) model gives a reasonable value for the gap of CuO (1.3 eV) (Ref. 29) and describes it as being a charge transfer gap: the highest $N-1$ state is essentially $d^9\underline{L}$ and the lowest (and only) $N+1$ state is mainly d^{10}. This is generally the case for the late transition-metal compounds. A better description of BIS requires consideration of a larger basis as we did for the densities of states displayed in Figs. 8 and 9, taking into account matrix elements[42] and the influence of electron energy losses.

IV. CONCLUSIONS

In conclusion we have shown that the electronic structure of the closed *d* shell Cu_2O compound is in good agreement with one-electron band-structure calculations, whereas for CuO the valence-band electronic structure is to a large extent dictated by electron-correlation effects. CuO, therefore, should be considered as a strongly correlated system in spite of the fact that the Cu $3d$–O $2p$ hybridization is extremely large. The band gap in CuO is found to be 1.4 eV and is caused by electron correlation, but it is of a charge transfer type since the *d*-*d* Coulomb interaction is considerably larger than the charge transfer energy. This puts CuO in phase *B* of the ZSA diagram.[24] The lowest ionization state in CuO is primarily of O 2*p* character which in a configuration interaction approach is a state of $|d^9\underline{L}\rangle$ character. However, the O 2*p* hole is strongly antiferromagnetically exchange coupled to a nearest-neighbor Cu (d^9) spin. An analysis of core satellite structure, valence- and conduction-band structure and two-hole states reached by Auger spectroscopy yield values of the relevant parameters: $U_{dd}(^1G) = A + 4B + 2C = 9.3$ eV and $U_{pp} = 4.6$ eV for Cu_2O; and $U_{dd}(^1G) = 7.8$ eV, $\Delta = 2.2$ eV, and $T(b_{1g}) = 2.3$ eV for CuO.

ACKNOWLEDGMENTS

We are grateful to O. Jepsen for making his results available before publication. This work was supported by the Netherlands Foundation for Fundamental Research on Matter (FOM), the Netherlands Foundation for Chemical Research (SON), and the Netherlands Organization for Scientific Research (NWO).

[1]A. F. Wells, *Structural Inorganic Chemistry,* 5th ed. (Clarendon, Oxford, 1984), p. 1120.

[2]S. Åsbrink and L. J. Norrby, Acta Crystallogr. Sect. B **26**, 8 (1970).

[3]M. T. Czyzyk and R. A. de Groot (unpublished).

[4]Band-structure calculations have been made recently by O. Jepsen and agree generally with those used in the present article (private communication).

[5]J. P. Dahl and A. C. Switendick, J. Phys. Chem. Solids **28**, 931 (1966).

[6]L. Kleinman and K. Mednick, Phys. Rev. B **21**, 1549 (1980).

[7]J. Robertson, Phys. Rev. B **28**, 3378 (1983).

[8]P. Marksteiner, P. Blaha, and K. Schwarz, Z. Phys. B **64**, 119 (1986).

[9]C. Kittel, *Introduction to Solid State Physics,* 5th ed. (Wiley, New York, 1976), p. 341; P. W. Baumeister, Phys. Rev. **121**, 359 (1961).

[10]J. R. Smith, J. G. Gay, and F. J. Arlinghaus, Phys. Rev. B **21**, 2201 (1980).

[11]F. P. Koffyberg and F. A. Benko, J. Appl. Phys. **53**, 1173 (1982).

[12]G. A. Sawatzky and J. W. Allen, Phys. Rev. Lett. **53**, 2339 (1984).

[13]K. Terakura, A. R. Williams, T. Oguchi, and J. Kuebler, Phys. Rev. Lett. **52**, 1830 (1984); K. Terakura, T. Oguchi, and J. Kuebler, Phys. Rev. B **30**, 4734 (1984).

[14]A. Rosencwaig and G. K. Wertheim, J. Electron. Spectrosc. **1**, 493 (1972/3).

[15]T. Robert, M. Bartel, and G. Offergeld, Surf. Sci. **33**, 123 (1972).

[16]K. S. Kim, J. Electron. Spectrosc. **3**, 217 (1974).

[17]L. Fiermans, R. Hoogewijs, and J. Vennik, Surf. Sci. **47**, 1 (1975).

[18]M. R. Thuler, R. L. Benbow, and Z. Hurych, Phys. Rev. B **26**, 669 (1982).

[19]J. A. Yarmoff, D. R. Clarke, W. Drube, A. Taleb-Ibrahimi, and F. J. Himpsel, Phys. Rev. B **36**, 3967 (1987).

[20]Very recently, inverse photoemission measurements have been done on CuO, with an electron beam energy of 16 eV. See A. J. Viescas, J. M. Tranquada, A. R. Moodenbaugh, and P. D. Robinson, Phys. Rev. B **37**, 3738 (1988).

[21]E. Antonides, E. C. Janse, and G. A. Sawatzky, Phys. Rev. B **15**, 1669 (1977); **15**, 4596 (1977).

[22]For a description of the ASW method, see A. R. Williams, J. Kübler, and C. D. Gelatt, Jr., Phys. Rev. B **19**, 6094 (1979); for the introduction of the ideal of localization, see O. K. Andersen and O. Jepsen, Phys. Rev. Lett. **53**, 2571 (1984).

[23]J. Zaanen, G. A. Sawatzky, and J. W. Allen, J. Magn. Magn. Mater. **54–57**, 607 (1986).

[24]J. Zaanen, G. A. Sawatzky, and J. W. Allen, Phys. Rev. Lett. **55**, 418 (1985).

[25]G. van der Laan, C. Westra, C. Haas, and G. A. Sawatzky, Phys. Rev. B **23**, 4369 (1981).

[26]S. Hüfner, G. K. Wertheim, and J. H. Wernick, Solid State Commun. **17**, 417 (1975).

[27]J. Zaanen, C. Westra, and G. A. Sawatzky, Phys. Rev. B **33**, 8060 (1986).

[28]G. A. Sawatzky, Stud. Inorg. Chem. **3**, 3 (1983).

[29]Zhi-xun Shen, J. W. Allen, J. J. Yeh, J. S. Kang, W. Ellis, W. Spicer, I. Lindau, M. B. Maple, Y. D. Dalichaouch, M. S. Torikachvili, J. Z. Sun, and T. H. Geballe, Phys. Rev. B **36**, 8414 (1987).

[30]H. W. Haak, G. A. Sawatzky, and T. D. Thomas, Phys. Rev. Lett. **41**, 1825 (1978); J. C. Fuggle, P. Bennett, F. U. Hillebrecht, A. Lenselink, and G. A. Sawatzky, Phys. Rev. Lett. **49**, 1797 (1983).

[31]J. J. Yeh and I. Lindau, At. Data Nucl. Data Tables **32**, 1 (1985).

[32]G. van der Laan, G. A. Sawatzky, C. Haas, and H. W. Myron, Phys. Rev. B **20**, 4287 (1979).

[33]A. Fujimori, F. Minami, and S. Sugano, Phys. Rev. B **29**, 5225 (1984).

[34]G. A. Sawatzky and D. Post, Phys. Rev. B **20**, 1546 (1979).

[35]D. van der Marel, J. van Elp, G. A. Sawatzky, and D. Heitmann, Phys. Rev. B **37**, 5136 (1988).

[36]D. van der Marel and G. A. Sawatzky, Phys. Rev. B **37**, 10674 (1988).

[37]C. E. Moore, *Atomic Energy Levels as Derived from the Analysis of Optical Spectra,* NBS Circular No. 467 (U.S. GPO, Washington, DC, 1958), 1949-1958.

[38]N. F. Mott and M. J. Littleton, Trans. Faraday Soc. **34**, 485 (1938).

[39]L. F. Mattheis, Phys. Rev. B **5**, 290 (1972).

[40]J. Zaanen, Ph.D. thesis, Groningen, The Netherlands, 1986 (unpublished); G. A. Sawatzky, in *Proceedings of the Tenth Taniguchi Symposium Core-Level Spectroscopy in Condensed Systems, Kashikojima, Japan, 1987,* edited by J. Kanamori and A. Kotani, Springer Series in Solid-State Sciences, Vol. 81 (Springer-Verlag, New York, 1988), p. 99.

[41]L. H. Tjeng, H. Eskes, and G. A. Sawatzky (unpublished).

[42]W. Speier, J. C. Fuggle, P. Durham, R. Zeller, R. J. Blake, and P. Sterne, J. Phys. C **21**, 2621 (1988).